SEISMIC MODELLING OF EMBANKMENTS ON SATURATED SOIL DEPOSITS.

L.M.N.Peiris, S.P.G.Madabhushi
& A.N.Schofield.

CUED/D-SOILS/TR300 (1996)

The contents of this report is a copy of the paper
published in the First International Symposium,
"EARTHQUAKE RESISTANT ENGINEERING STRUCTURES 96",
Greece, 1996.

Seismic modeling of embankments on saturated soil deposits.

S.P.G. Madabhushi*, L.M.N. Peiris+ & A.N. Schofield+
**University of Edinburgh, U.K.*
+ *University of Cambridge, U.K.*

Abstract.

Following an earthquake it is important that the transport networks are operable for the use of relief convoys. Following the Northridge earthquake several of the key road networks in the Los Angeles area have become unusable. Kobe earthquake presented a similar problem to the transport networks. Embankments constitute a key element in highways and other transport networks. It is therefore important to ensure the safety of embankments subjected to seismic loading. This paper presents the results of the centrifuge tests carried out as a preliminary investigation into the behaviour of granular embankments founded on loose saturated sand subjected to earthquake loading. It was observed that the embankment settled by considerable amounts during the earthquakes. The post test investigation revealed that gravel had sunk into the sand foundation and there was some lateral spread of the embankment.

1 Introduction.

During an earthquake event embankments founded on saturated sandy soils suffer a risk of liquefaction induced failure. This paper concerns itself with the study of dynamic performance of embankments situated on saturated sand beds using the centrifuge modeling technique. Schofield (1980, 81) discussed the scaling laws which relate the behaviour of a model in earthquakes to the prototype behaviour in the field. Over the past decade, dynamic centrifuge techniques has established itself as a useful tool for the geotechnical engineer to investigate earthquake induced failures. Schofield and Lee (1988) explain the decoupling of the crest of a sand island from the input earthquake following liquefaction of the foundation soil. Habibian (1987) studied the seismic behaviour of Venezuelan coastal dykes situated on saturated sand beds.

Venter (1988) used an embankment carved from a solid block of wood/dural in his dynamic centrifuge tests.

This paper describes the behaviour of a gravel embankment founded on loose saturated sand subjected to seismic loading. The embankment was made of gravel of average diameter of 10mm and the foundation was made from Leighton Buzzard LB 100/170 sand at a relative density of approximately 40% and saturated with silicone oil of viscosity 50 centistokes as dictated by the scaling laws. Four earthquakes of medium strength were fired at a frequency of 95Hz at 50g centrifuge acceleration. A considerable crest settlement was observed during the earthquakes due to pore pressure rise reaching near liquefaction in the foundation underneath the embankment. Post test investigation revealed that the embankment gravel had migrated into the fluidized sand under the embankment, being the predominant failure mechanism during the earthquakes. Several other failure mechanisms were also highlighted.

2 Equipment & experimental procedure.

2.1 Centrifuge Scaling Relationships.

Fig 1. shows a model of a block of soil and its corresponding prototype. Constructing a model with dimensions scaled by l/N and subsequently increasing the acceleration by a factor N leads to identical stresses at the homologous points in the model and the prototype. This similarity ensure that the soil .behaviour of the model and the prototype are unchanged. Table 1 shows a summary of the scaling laws.

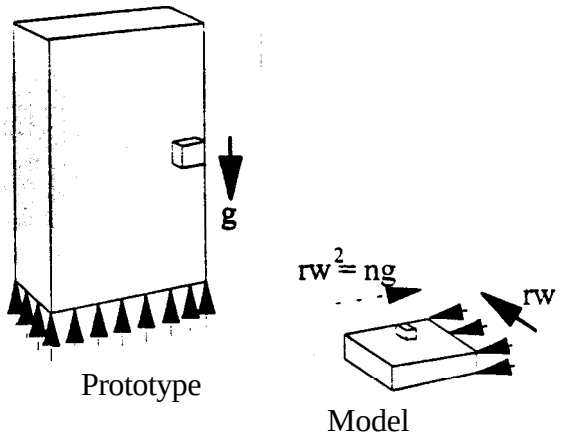

Fig. 1 Centrifuge model and prototype.

Table 1 Summary of scaling laws.

Event type	Quantity	Model/ Prototype ratio
General	Stress	1
	Strain	1
	Length	1/N
	Area	1/N²
	Volume	1/N³
	Mass	1
	Force	1/N²
Dynamic	Time	1/N
	Frequency	N
	Velocity	1
	Acceleration	N
	Strain rate	N

Schofield (198 1) points out that if accelerations in the model are N times larger and the length dimensions are N times smaller than the prototype, then from dimensional analysis, it can be concluded that the dynamic events occur N times faster, i.e. time is reduced by a factor of N and frequency of shaking is N times larger in the model. Hence the base shaking of form $x_p = a \sin(\omega t_p)$ at prototype scale is described by $x_m = a/N \sin[(N\omega)t_m]$ in the model. Differentiating once would give identical velocities for both model and prototype. Differentiating twice gives both the amplitude and frequency of acceleration N times larger in the model than in prototype.

Since dynamic events occur N times faster in model than prototype, the rate of pore pressure generation is also N times large. However the rate of dissipation is N^2 times faster in model than in prototype for the same soil and pore fluid used in both prototype and model. This is apparent by looking at the diffusion equation for pore pressure, u given here in one dimension for clarity

$$\nabla^2 u = (1/C_v)\, \partial u/\partial t$$

where C_v is coefficient of consolidation, and is the same for both model and prototype provided the same soil and pore fluid are used. To eliminate this discrepancy, a pore fluid N times viscous than prototype pore fluid is used in model thereby reducing the rate of dissipation from N^2 to N times that in the prototype matching with the generation rate.

2.2 Bumpy Road Actuator

The centrifuge tests were conducted on board the Cambridge University Geotechnical Centrifuge, Schofield (1980) and earthquakes fired using the bumpy road actuator, Kutter (1982). Fig. 2 shows a cut-away view of the bumpy road shaker.

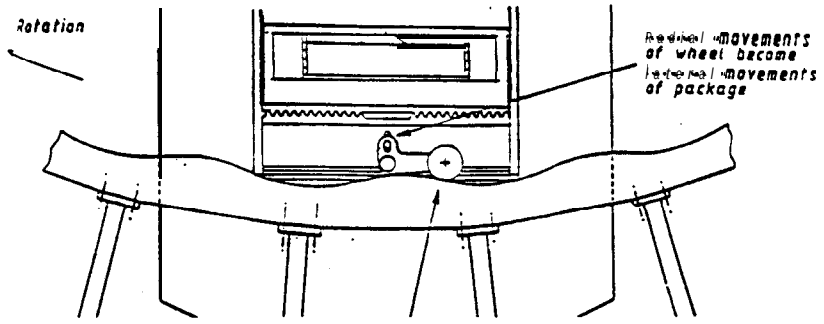

Fig. 2 Cut-away view of the bumpy road shaker.

As the centrifuge spins up, the package swings up and sits on the rack. A sinusoidal track with 10 cycles is firmly mounted onto the wall of the centrifuge chamber. An event is triggered by moving the wheel on to the track with pressure controlled across a double acting piston. The wheel can be

made to come in to contact with the track once and once only during any particular loading event. The radial movement of the wheel is translated into lateral movement of the base of the package by a bell-crank mechanism. A slider offset mechanism will allow the earthquake strength experienced by the package to be varied. At 50g centrifuge acceleration, the track produced 10 cycles of roughly sinusoidal shape with a model frequency of 95Hz corresponding to 1.9Hz in prototype.

2.3 Model Container.

The model container used was the Equivalent Shear Beam (ESB) box, Zeng (1991), Madabhushi (1994), of internal dimensions 560 x 250 x 200mm (length x width x height), designed to give a semi-infinite soil model which would eliminate the dissimilarity in the boundary conditions between model and the prototype. This box would satisfy stress and strain similarity and suppress p-wave generation at the model boundaries. Fig. 3 shows a 3-D view of the box along with its lid.

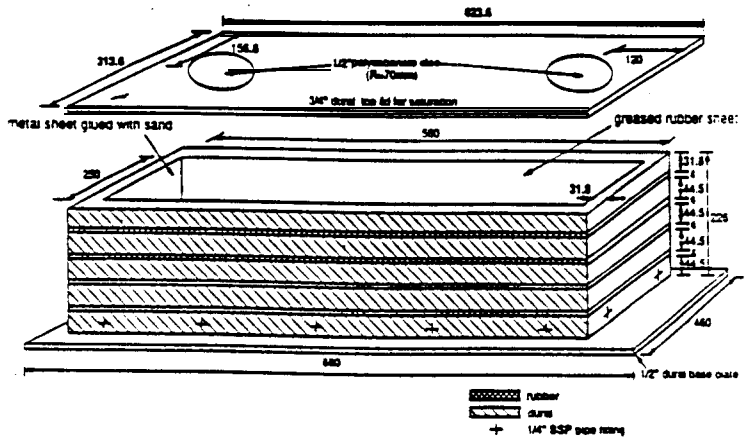

Fig. 3 A 3-D view of the Cambridge Equivalent Shear Beam (ESB) container.

2.4 Model Preparation.

Sand used as the foundation material is Leighton Buzzard LB 100/170 fine sand. Table 2 shows the properties of LB 100/170 sand. Sand was air pluviated into the ESB box using a sand hopper held at a fixed height above the surface of the sand inside the model as pouring took place to obtain a sample of uniform relative density. The final depth of the sand model was 180mm and estimated to have a relative density, Dr of around 40%. In prototype scale the sand depth is 9m since the test was carried out at 50g centrifuge acceleration. The foundation was instrumented with accelerometers (ACCs) and pore pressure transducers (PPTs) as shown in fig. 4. The locations of transducers are given in table 3. After sand piuviation, the model was saturated with 50

centistokes silicone oil under a vacuum of -28inHg. Properties of silicone oil are given in table 4. Silicone oil was used as the pore fluid in order to satisfy the similarity in the centrifuge scaling relationships as mentioned earlier. The embankment was constructed after saturation by slowly pouring gravel onto the surface of the sand keeping the pouring height as low as 20mm so that gravel will fall into place to form a loose embankment with an approximately triangular profile as shown in fig. 4. The embankment was -120mm wide and -50mm high taking up the full width of the ESB box longitudinally. In protoytpe scale, this corresponds to an embankment of width 6m and height 2.5m. Gravel used had an average diameter of 10mm and an irregular surface. A camera was mounted facing the embankment at an angle to its longitudinal axis so that any settlment can be observed in flight.

Table 2 Summary of the properties of 1001170 Leighton Buzzard sand.

D 10 grain size	0.095 mm
D_{50} grain size	0.14 mm
D_{60} grain size	0.15mm
Specific Gravity G_s	2.65
Minirnurn voids ratio e_{min}	0.613
Maximum voids ratio e_{max}	1.014
Permeability to water (e=0.72)	0.98E-4 m/s
Estimated angle of shearing Resistance at critical state ϕ_{crit}	32"

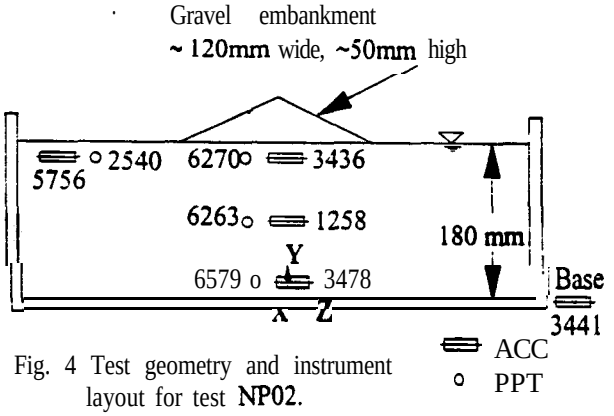

Fig. 4 Test geometry and instrument layout for test NP02.

Table 4 Some properties of silicone oil.

Specific gravity at 25°	0.96
Viscosity temp. coeff.	0.6cs/Kelvin
Volumetric expansion coeff.	0.096%/C
Boiling point	200°C at 2 mmHg
Bulk modulus (up to 1000kPa)	750000 kPa

Table 3 Locations of instruments.

Instrm. I.D.	Coordinate (mm)		
ACCs	x	Y	Z
3441	-125	0	-300
3478	-1	40	-20
1258	-12	103	-10
3436	-16	148	-11
5756	-4	152	-252
PPTs			
6579	-7	38	42
6263	2	100	39
6270	-18	147	50
2540	13	148	-196

2.5 Test Procedure.

After the model preparation was completed the model package was mounted onto the beam along with its counterweight and the centrifuge beam was accelerated to 50g. Few minutes after reaching 50g an earthquake was fired with data being recorded on computer and on Racal recorders. Static pore pressure readings were taken after allowing time for consolidation. In this

way, all four earthquakes were fired after which the centrifuge was stopped. The earthquakes fired were of medium strength with a frequency of 95Hz and had just over 10 cycles.

3 Test results & analysis.

3.1 Experimental observations.

Figs. 6 & 7 shows the accelerometer and excess pore pressure transducer data obtained in the first and the fourth earthquakes fired. The first earthquake had a package peak strength of 36.25% of 50g recorded on ACC3441. All accelerations are given as percentages of the centrifuge g level. Subsequent earthquakes fired were of similar strengths at 42.49% as shown in fig. 7 in the case of the fourth earthquake. The accelerometers along the centerline of the model underneath the embankment indicates a reduction in strength as the earthquake progressed. In EQ1 ACC3436 had a reduction in the acceleration after four cycles whereas in EQ4 this happened after two cycles. This degradation in strength occurs quickly in the upper layers closer to the embankment. The ACC traces also indicates an amplification of strength from the base of the model to mid-depth and then an attenuation to the surface. For example in the first earthquake, ACC3478 registered a peak strength of 19.5% which rose to 2312% in ACC1258 and then dropped to 8.5% as indicated by the reading on ACC3436. A similar pattern was also observed in all other earthquake. The accelerometer located away from the embankment, ACC5756 followed the bumpy road motion reaching accelerations much higher than ACC3436 which is at the same level but underneath the embankment.

The pore pressure transducer PPT6579 located near the base of the model indicated a rise in excess pore pressure and almost reaching a plateau in all earthquakes. In the first earthquake, under the embankment, the mid-depth and the near surface PPTs indicated a cyclic rise of pore pressure whereas in the fourth earthquake, this cyclic rise was only observed in PPT6270 just below the embankment. Pore pressure ratio r_u is defined as the ratio of excess pore pressure generated and the initial effective stress where the initial effective stress was calculated as stated in the next section. The ratios r_u along the model centerline are 0.7 at base, 0.8 at mid-depth and 0.4 near the embankment/foundation interface for the first earthquake. This indicates that the mid-depth was close to liquefaction. For the fourth earthquake the ratios are 0.8 for base, 0.6 for mid-depth and 0.5 near the embankment/foundation interface indicating that the base of the model was close to liquefaction.

Another phenomenon observed was the phase shifts in the accelerometer traces under the embankment. In the first earthquake, ACC3436 shows a distinct phase shift compared to ACC3478 with the third and fourth

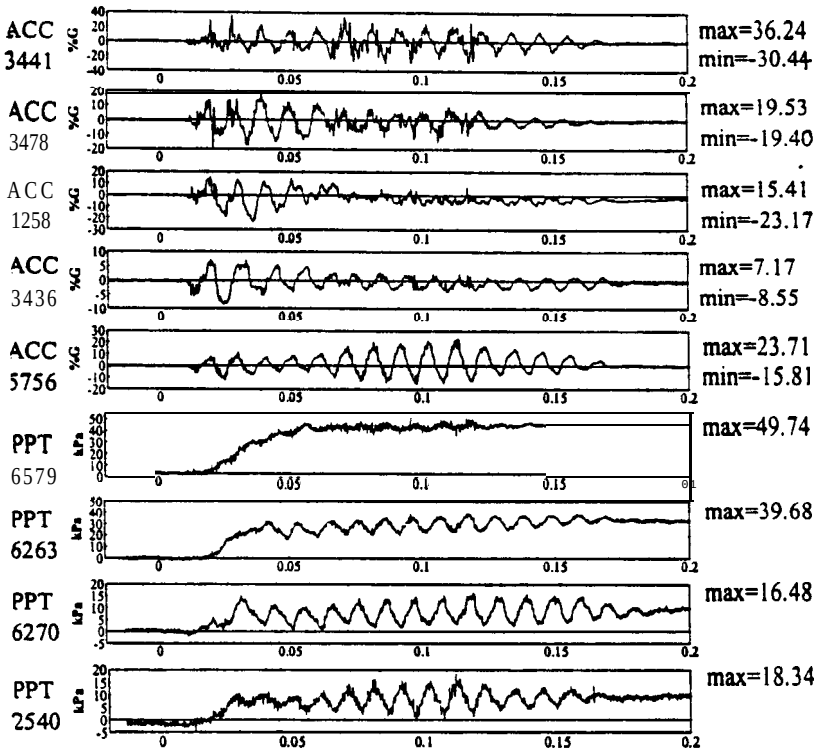

Fig.6 Short term time records for earthquake no. 1 of test NP02.

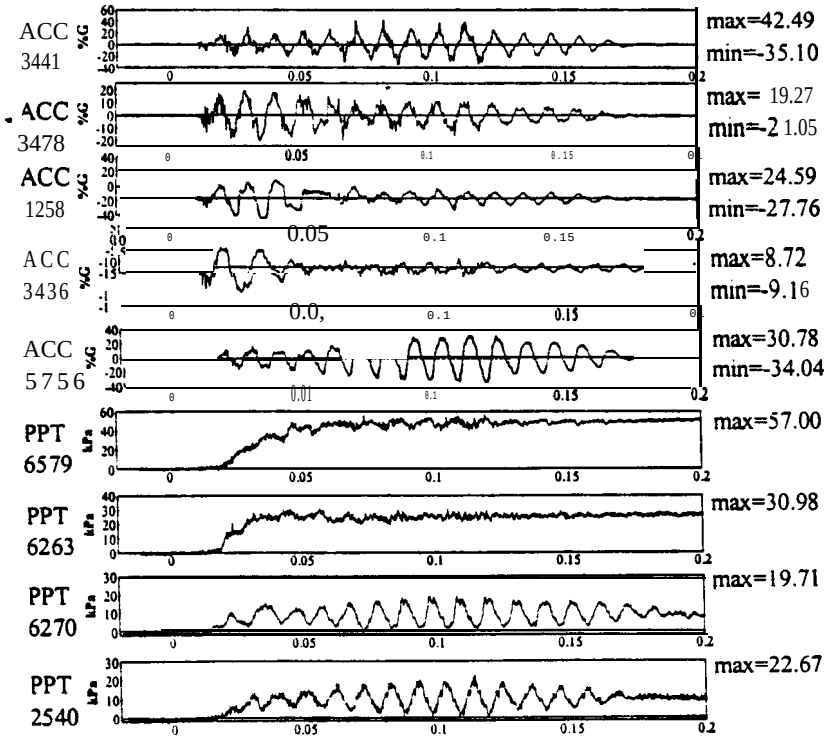

Fig.7 Short term time records for earthquake no.4 of test NP02.

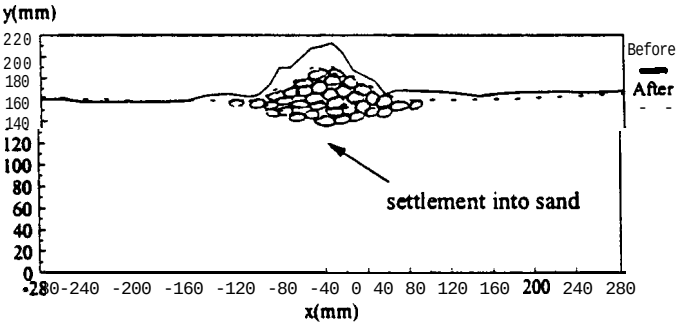

Fig. 8 Initial and final profiles of test NP02.

peaks of ACC3436 remaining to the right of that of ACC3478. Also the peaks are flattening. This phase shift is more clear in the fourth earthquake which is of high strength, where the second peak of ACC3436 is almost 180" out of phase compared to that of ACC3478. These phase shifts points out to decoupling of the sand foundation that existed as the pore pressures rose.

During all the earthquakes, the embankment crest settled by a significant amount giving an overall settlement of 22mm in model scale corresponding to 1. lm settlement in prototype (see fig. 8). For any one earthquake this represents a crest settlement of 27.5cm (=1. 1m/4) in prototype. During the first earthquake there was lateral spread of the embankment with gravel rolling along the slope. The slope of this embankment is 39.8" which is close to the typical angle of repose of gravel of 10mm diameter, at 35" to 40". This means that gravel on the slope of the embankment are unstable and hence they roll down, spreading the embankment to reach equilibrium. The main mechanism of settlement in all four earthquakes was due to gravel settling in a sand foundation which is experiencing a rise in pore fluid pressure. Post-test investigation revealed that the gravel particles had migrated downward to a depth of 30mm in the model as shown in fig. 8. This corresponds to a 1.5m migration in a 9m foundation in prototype. Settlement also occured due to consolidation of foundation after an earthquake and due to densification within the embankment when gravel particles rearrange themselves.

3.2 Estimation of the crest settlement.

Let us assume that the embankment is made of deformable material and sitting on an elastic foundation with constant stiffness. The embankment is 6m wide, 2.5m high and 12.5m long and the foundation is of depth 9m. The initial effective vertical stress is given by (Terzaghi (1943)),

σ_v' = due to foundation soil + due to linearly increasing load of embankment
(kPa)

$$\sigma_v' = 8.732\, z + 23.316 \tan^{-1}(3/z) \qquad (1)$$

where z is the depth below foundation surface.
The initial horizontal effective stress is similarly defined as

$$\sigma_h' = 8.732\ z * K_o + \text{due to linearly increasing load of embankment}$$

Where $K_o = 1 - \sin \Phi'$

Therefore,

$$\sigma_h' = 4.105\ z + 23.3\ 16\ (\tan\text{-}'(3/z) - (z/3) \ln \{(9/z') + 1\} \qquad (2)$$

The maximum shear modulus as stated by Hardin & Dmevich (1972) is,

$$Gmax = 100\ \{ [3\text{-}e]^2/[1+e]\} * (\sigma_m')^2 \qquad (3)$$

where e is the void ratio and σ_m' is the mean effective stress given by,

$$\sigma_m' = (\sigma_v' + 2\sigma_h')/3 \qquad (4)$$

The Youngs modulus is given by,

$$E = 2G\ (1 + \nu) \qquad (5)$$

where v = 0.5 for undrained and 0.2 for drained.
The embankment crest settlement is given by,

$$\delta_c = (\sigma_{em} / E) * 9 \qquad (6)$$

where σ_{em} is the stress at the center of the embankment/foundation interface due to the linearly increasing load obtained from eqn. (1) with z = 0. Using eqns. (1) to (5) and evaluating at z = 4.5m (mid depth) gives a drained Young's modulus for the foundation of 3296.9 kPa prior to earthquakes. Using eqn. (6) gives a settlement of O.lm in prototype corresponding to 2mm in model. During the first earthquake, the pore pressure at the mid-depth rose to 39.685 kPa as indicated by PPT6263 in fig. 6. Using the new effective stresses calculated by substracting the pore pressure from the initial effective stress values gives an undrained Young's modulus of 1570.8 kPa. It is assumed that the foundation is undrained throughout the earthquake. This gives a settlement of 0.21m in prototype or 4mm in model during the earthquake. The overall crest settlement including the initial crest settlement and assuming that each earthquake gave the same crest settlement, is 18mm in model and 0.9m in prototype. This is comparing with the observed 22rnm in model and 1.1 m in the corresponding prototype. The discrepancy in the estimated and the observed values comes from the consolidation of the foundation which takes place after each earthquake causing further crest settlement.

4 Concluding remarks.

Tests were carried out as a preliminary investigation into the behaviour of gravel embankments founded on loose saturated sand. It was discovered that when the shear waves propagated, pore pressure underneath the embankment rose in some regions approaching fluidization or liquefaction. Pore pressure ratios as high as 0.8 were recorded at mid-depth in the first earthquake causing the decoupling that was observed in the accelerometers buried in the foundation. This pore pressure rise had softened the sand foundation hence the bearing capacity leading to the settlement of the embankment as the gravel particles migrated into the foundation. The migrated distance was 1.5m in a 9m foundation leading to a crest settlement of l.lm in all four earthquakes. The crest settlment was estimated using an elastic analysis with the stiffhess degradation accounted for due to pore pressure rise. This yielded an overall settlement of 0.9m for all four earthquakes which is close to that observed, although without calculating the consolidation settlement. Lateral spread of the embankment largely contributed to the crest settlement only during the first earthquake with additional contributions coming from foundation consolidation and densification within the embankment.

References.

Habibian, A. *Seismic modellin o coastal dykes on layered sand foundations,* PhD thesis, Cambridge University,a. .,d1987.

Hardin, B.O. & Dmevich, V.P. Shear modulus and damping in soils: design equations and *curves. Journal of Soil Mechanics and Foundation Engineering Division, ASCE,* 1972, No.SM7, 667-692.

Kutter, B.L. *Centrifugal modelling of the response of clay embankments to earthquakes,* PhD thesis, Cambridge University, U.K., 1982.

Madabhushi, S.P.G. *Dynamic response of the Equivalent Shear. Beam (ESB) container.* Technical Report, CUED/D-SOILS/TR270, Cambndge University, U.K., 1994.

Schofield, A.N. Cambridge Geotechnical Centrifuge Operations, *Geotechnique,* 1980, 25, No.4, 743-76 1.

Schofield, A.N. Dynamic and Earthquake Geotechnical Centrifuge Modelling, pp. 1081-l 100, *Proceedings of Int. Con on Recent Advances in Geo. Earth. Eng. and Soil Dynamics,* St. Louis, Missouri, 1981.

Schofield, A.N. & Lee, F.H. Centrifuge modelling of sand embankments and islands in earthquakes, *Geotechnique,* 1988, 38, No.10, 455-58.

Terzaghi, *K. Theoretical Soil Mechanics,* John Wiley & Sons., New York, 1943.

Venter, K.P. *Modelling the response of sand to cyclic loads,* PhD thesis, Cambridge University, U.K., 1988.

Zeng, X. *Design of the Cambridge Dynamic Shear Box.* Technical Report, CUED/D-SOILS/TR241, Cambridge University, U.K., 1991.